Probabilistic Analysis of Process Chain "Forming to Crash" Regarding Failure Prediction

Burak Özarmut[1], Helmut Richter[1], Alexander Brosius[2]

[1]*ThyssenKrupp Steel Europe AG, Dortmund*
burak.oezarmut@thyssenkrupp.com & helmut.richter@thyssenkrupp.com

[2] *Institut für Fertigungstechnik, Formgebende Fertigungsverfahren, Technische Universität Dresden, Dresden, alexander.brosius@tu-dresden.de*

Abstract

Numerical analysis of forming and crash processes is usually carried out deterministically. However, the variations of the parameters describing materials and processes cause significant deviations in the prediction quality. This observation becomes more important if the failure prediction in process chains like forming to crash is considered. Usually, the material and process parameters are identified by means of an inverse or a direct identification procedure using experimental data. Nevertheless, the identification process itself contains uncertainty, as mean values are usually utilized for this purpose. It is therefore not known whether the process simulated with the identified parameters is robust and how the variation of parameters influences the quality of failure prediction. Stochastic analysis, replacing the parameters with stochastic distributions, can be performed to find out the variation of outputs due to the variation of input parameters. Since the computational cost of such an analysis would be too high to carry out using only FE simulations, it is performed on metamodels generated with relatively few FE simulations. Assuming the generated metamodel is accurate enough, reliable sensitivity information can also be obtained through methods such as Anova and Sobol Indices. The optimization and probabilistic analysis software LS-Opt serves as an efficient tool to conduct such study.
In this paper, parameters of a high strength steel grade, used mainly in the automotive industry, are replaced with distribution functions reflecting the real deviations of material and process parameters. A suitable sampling algorithm for the selected metamodeling technique is then used to generate parameter sets for the FE simulations. In order to keep the computational cost as low as possible, some simplifications and assumptions have been made concerning the hardening and strain rate dependency. The statistics of the desired outputs and the influence of the material and process parameters are computed by means of the metamodel. The results show that the variation of modeling parameters such as fracture curve, hardening, and plasticity, causes higher amount of variation on the failure prediction indicators like displacement up to fracture. Furthermore, it has also been found that the standard deviation of results increases with the increasing element size pointing out the importance of reducing uncertainty in the methods used for defining model parameters if coarser meshes are to be used.

Keywords:
Probabilistic analysis, ANOVA, Sobol Indices, Gissmo, CrachFEM, Fracture modeling, Crash simulation, Strain rate sensitivity, Modified Johnson-Cook

1 Introduction

The material and model parameters used to describe the processes in the process chain are essential to find an accurate representation of deformation and failure. They can be classified into the following groups

- Material description (hardening, strain rate, anisotropy, etc.)
- Modelling influence (mesh fineness, discretization, element type, etc.)
- Model calibration (scatter of fracture data, failure evolution, non-linearity of test path, etc.)

Since the calibration of model parameters is accomplished by means of experimental results having relatively high uncertainty, they are prone to deviate and might be misleading. Therefore, it would be beneficial to identify the most important uncertainties, quantify them and compute their contribution on the desired outputs. Deterministic simulations can give us a hint about one possibility that the system might undergo and other possibilities are left out, but there might still be many scenarios to pay attention to. Analyzing the process chain considering stochastic aspects can provide information on how robust the processes are and what to regard more important while modeling them.

In the current work, a methodology for analyzing the process chain taking stochastic aspects into account has been developed. Forming and crash steps are investigated individually, but focus is given more on the variation of failure prediction at the crash step due to variation of input parameters. The developed methodology is tested on an analytical example followed by quasi-static and dynamic analysis of two different parts under 3-point bending.

2 Methodology for the Probabilistic Analysis of Process Chain "Forming to Crash"

Stochastic simulations, Fig. 1, are based on the idea of solving mathematical problems using random input parameters, which are conceived as the influential parameters of the simulations. In a stochastic simulation, the parameters that might influence the output of a deterministic simulation are replaced with stochastic distributions to take uncertainties into account. For the purpose of performing stochastic simulations, there are some methods available. Monte Carlo methods are the most famous ones among them. They are defined simply as computational algorithms used to construct stochastic models rather than deterministic models.
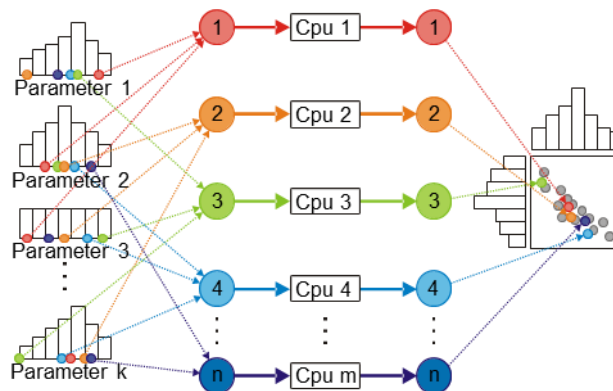

Fig.1: Schematic representation of a stochastic simulation, acc. to [1]

Quantifying uncertainties and computing their contribution on the desired outputs are based on integrations in possibly high-dimensional design space of input parameters, which would make Monte Carlo analysis computationally too expensive to carry out using only FE simulations. However, the computational cost can be dramatically reduced by applying approximation models, known as metamodels or surrogate models. Metamodel-based Monte Carlo analysis is a 2 step process [2], illustrated in Fig.1.

1. The FE simulations are performed according to the points generated by the sampling algorithm. The sampling algorithm takes bounds and constraints into account. This step is used for building metamodels as accurate and representable as possible. Therefore, the choice of sampling algorithm and metamodel type plays a crucial role.

2. Millions of function evaluations are performed on the metamodel. Points are selected considering statistical distributions. Uncertainty quantification, stochastic contribution and global sensitivity analyses are carried out in this step.
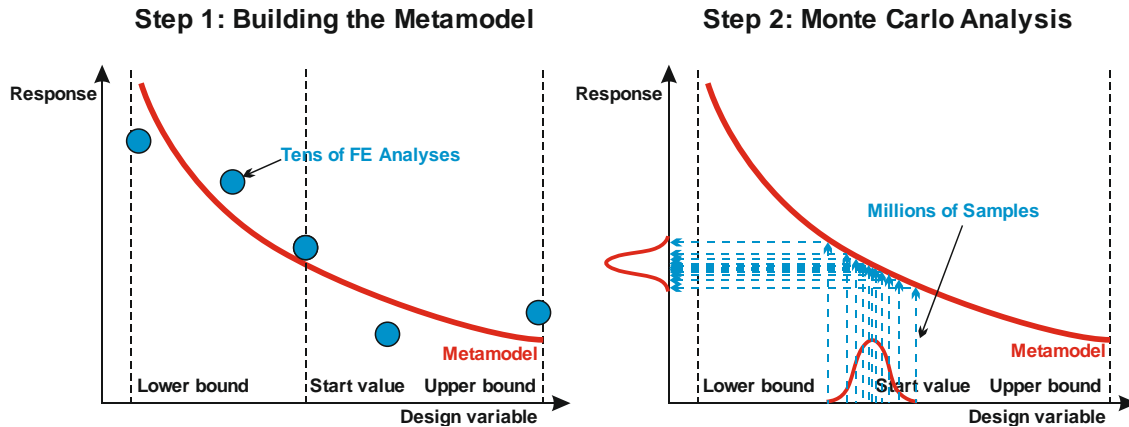

Fig.2:   Metamodel based Monte Carlo Analysis in 2 steps, acc. to [2]

As the reliability of results depends on the accuracy of the metamodel, it is required to perform as many FE simulations as necessary to construct an accurate metamodel. Nevertheless, estimating the number of required simulations beforehand is not an easy task. Herein, augmentation of an existing design can help to increase the metamodel accuracy. The chosen sampling algorithm must consider the previous points and add new ones efficiently in the design space. Space filling algorithm, suitable for this kind of study and available in LS-Opt, has been utilized in this work. The procedure then becomes as follows:

1. Generate 2*n+1 (n is the number of variables) number of sampling points using Space-Filling algorithm and perform the corresponding FE simulations.
2. Build metamodel and check its accuracy with some very well-known accuracy measures, such as residual sum-of-squares, predicted sum-of-squares residual, coefficient of multiple determination, and average error. If the desired accuracy is not reached, turn back to the first step.
3. Perform Monte Carlo analysis by means of the generated metamodel.

The global sensitivity measures ANOVA and SOBOL indices will be used for revealing linear and non-linear relations between parameters and responses. They will be briefly explained in the following subsections.

2.1   ANOVA

ANOVA is a method for modeling the relationship between two or more independent variables and a dependent variable. The multi variate linear regression model describes how the mean value of a response changes w.r.t. the variables. It is defined for the response y_i as follows:

$$y_i = b_0 + \sum_{j=1}^{n} \frac{b_j}{\Delta x_j} x_j \tag{1}$$

where i is the number of responses and n is the number of variables [3].
The regression coefficients b_j are related to the importance of variables, whereas Δb_j describes the confidence interval of the corresponding regression coefficient. The significance of variables is determined through a partial F-test (equivalent to Student's t-test) [4]. Apart from the significance, it is also possible to define the correlation type between variables and responses by means of ANOVA. Another advantage of ANOVA over SOBOL indices is that it provides the absolute change of the mean value of a response. On the other hand, only linear relations can be revealed by ANOVA.

2.2   SOBOL Indices

The SOBOL indices are known as global sensitivity indices that quantify the influence of a variable on an output by variance decomposition. In other words, it is simply a ratio of the expected variance caused by a variable to the total variance caused by all variables taken into account. They are generally applicable non-linear sensitivity measures. All sensitivity indices $S_{i,i=1,...,n}$ are nonnegative

and their sum is equal to 1. The normalized sensitivity measure S_i for a model parameter $x_{i,i=1,2,...,n}$ is given by:

$$S_i = \frac{\widetilde{S_i}}{\sum_{j=1}^n \widetilde{S_i}} \tag{2}$$

where $\widetilde{S_i}$ represents the influence of x_i on the model response according to a specific sensitivity measure [2]. Accordingly, the importance ranking of the variables is determined w.r.t. the indices indicating individual contribution of variables on the total variance of a model response. On details of global sensitivity analysis by means of the Sobol indices and how they are calculated it is referred to [5, 6]. The biggest advantage of Sobol indices over ANOVA is the possibility of performing both linear and non-linear analysis. Moreover, the indices can be directly comparable as they are normalized values. This property makes it also independent from the range of variables.

It should also be pointed out that the Sobol indices are also computed for performing the Stochastic Contribution Analysis in LS-Opt, which takes the distribution functions of the parameters into account, whereas it is not the case for the Global Sensitivity Analysis.

3 Material Characterization

In this section, the numerical models describing hardening, yield locus and damage behavior of the material used for this work are briefly explained. Details on the optimization methods, conducted mechanical tests, and features of the models can be found in [7]. The parameters of the optimized models constitute the mean values for the Monte Carlo analysis.

3.1 Extrapolation of quasi-static and dynamic yield curves

In crashworthiness evaluations it is expected to have much higher plastic strains compared to the tests utilized for defining the hardening behavior of materials. This makes the modeling and thereby extrapolation of yield curves an important source of uncertainty in the validation process. Throughout this work, the Swift approximation is used to express flow stress in terms of equivalent plastic strain.

$$\sigma_{y_0} = K * (\varepsilon_0 + \varepsilon_p)^n \tag{3}$$

The material constants, the strength coefficient K, the hardening exponent n and ε_0 representing the elastic strain at yield are identified through inverse parameter identification using the pre-necking part of a force vs. displacement curve of a uniaxial test. With its relatively less number of parameters compared to a usually applied mixture law, i.e., linear combination of the Swift and Hockett-Sherby laws, it is suitable for investigating the uncertainty caused by the variation of experimental yield curves via metamodel based analysis approaches.

Crashworthiness tests are highly dynamic deformation processes, which can differ notably from those that occur at low strain rates like quasi-static ones. This revealed the need for numerical models that can describe the hardening behavior of materials under dynamic loading conditions. [8] has proposed a model, widely known as Johnson-Cook, to consider not only strain rate but also temperature dependency with adiabatic assumption. [9] modified the linear expression of its strain rate hardening term into exponential expression, and [10] found that the exponential term makes the model more suitable to DP600, similar to DP800 used in this work. The modified Johnson-Cook model is coupled with the Swift approximation and has been implemented as a parameterized table to describe the strain rate dependency in this work.

$$\sigma_y = \sigma_{y_0} * \left[1 + C\left(ln\frac{\dot{\varepsilon}}{\dot{\varepsilon}_0}\right)^p\right] \tag{4}$$

There are two material constants, C and p, but only the coefficient C will be varied during the probabilistic analysis. Fig. 3 demonstrates the yield stress change w.r.t. strain rate. The yield curves of high strain rates were smoothened. The identified parameters together with the damage model were validated using the force vs. displacement curve of a high speed tensile test. As shown in Fig. 3, the resulting force vs. displacement curves are in good agreement. Since the approximation of the quasi-static yield curve is used as reference and for the modified Johnson-Cook model, the yield strengths of the dynamic yield curves are not met correctly. Knowing that very high localized plastic strains take place in the crash step, this modeling discrepancy is not expected to alter the results substantially.
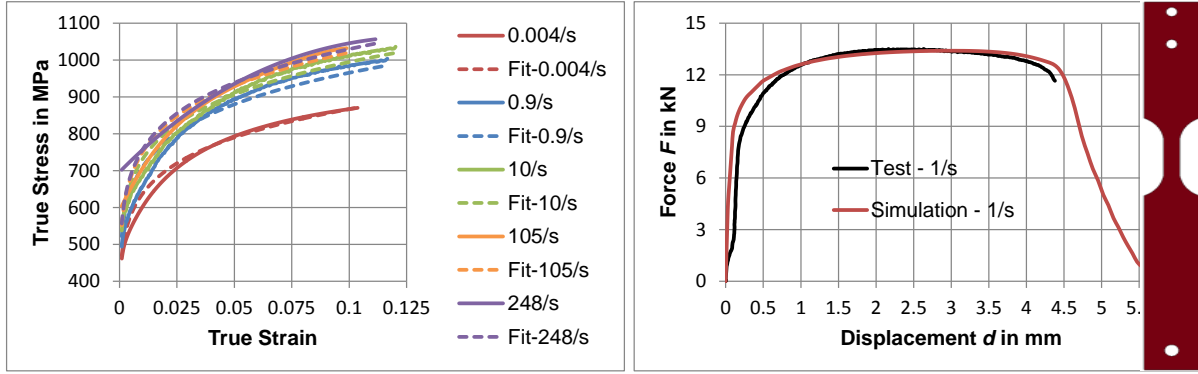
Fig.3:   *Strain rate dependent yield curves and their fit by means of the modified Johnson-Cook model (left) and validation of a high speed tensile test with the optimized and fitted parameters (right)*

3.2   Yield Locus

Crash simulations are mostly performed with an isotropic yield criterion, but defining the initial yield locus as representative as possible might deliver more accurate results [11]. In order to investigate how the variation of model parameters influences the outputs of crash simulations, 2 elasto-plastic material models have been employed. The first yield criterion is von Mises, which is defined for plane stress state as

$$\sigma_y = \sqrt{\sigma_1^2 + \sigma_2^2 - \sigma_1\sigma_2} \tag{5}$$

The second yield criterion, YLD2000-2D [12], is a complex one consisting of totally 9 parameters, namely the $\alpha_{i,i=1...8}$ values and the flow exponent m. The yield function is based on 2 linear transformations of the Cauchy Stress tensor and is expressed as

$$\varphi' + \varphi'' = 2\sigma_y^m \tag{6}$$

where φ' and φ'' are defined as

$$\varphi' = |X_1' - X_2'|^m \quad \varphi'' = |2X_2'' - X_1''|^m + |2X_1'' - X_2''|^m \tag{7}$$

The linear transformations of the stress tensors ($\boldsymbol{X'}$ & $\boldsymbol{X''}$) are

$$\boldsymbol{X'} = \boldsymbol{C'} \cdot \boldsymbol{s} = \boldsymbol{L'} \cdot \boldsymbol{\sigma} \quad\quad \boldsymbol{X''} = \boldsymbol{C''} \cdot \boldsymbol{s} = \boldsymbol{L''} \cdot \boldsymbol{\sigma} \tag{8}$$

In equation 8, $\boldsymbol{s}$ and $\boldsymbol{\sigma}$ refer to the deviatoric and Cauchy stress tensors, whereas $\boldsymbol{C'}$, $\boldsymbol{C''}$, $\boldsymbol{L'}$, and $\boldsymbol{L''}$ imply the employed transformers. The tensors $\boldsymbol{L'}$ and $\boldsymbol{L''}$ as functions of the anisotropy coefficients $\alpha_{i,i=1...8}$, i.e.,

$$L_{ij}' = f(\alpha_1, ..., \alpha_n) \text{ with } i,j = 1,2,3 \ \& \ n = 8 \tag{9}$$

$$L_{ij}'' = f(\alpha_1, ..., \alpha_n) \text{ with } i,j = 1,2,3 \ \& \ n = 8 \tag{10}$$

The α values and the exponent m are identified with the methodology explained in [7]. Fig. 4 shows the normalized yield loci.
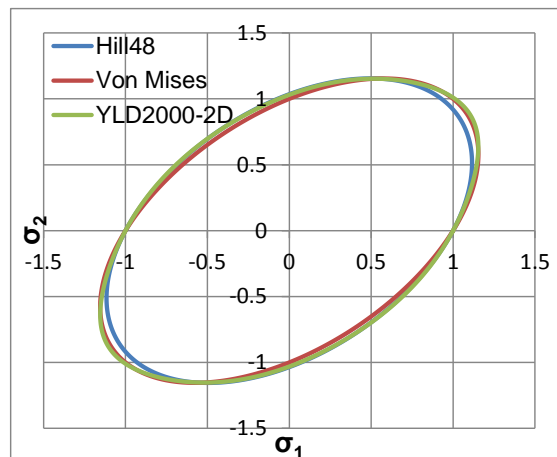

Fig.4:   *Comparison of different yield loci for the utilized material*

3.2.1 Influence of YLD2000-2D parameters regarding plane strain & biaxial stress states

Thorough investigation of the numerical examples utilized in this work revealed that the plane strain and biaxial stress states govern the failure of the tested parts. For this reason, it makes sense to focus on the parameters influencing mostly the mentioned quadrants of the yield locus in the Monte Carlo analysis. Accordingly, it is intended to reduce the computational cost by reducing the dimension of the problem. In order to find out the most important anisotropy parameters, a parameter study was carried out considering only the mentioned stress states and the yield locus w.r.t. the rolling direction. The yield locus was computed for 0°, 45° and 90° w.r.t. the rolling direction assuming 0° coincides with it. Upon increasing each parameter by 10% individually, the yield locus was recomputed considering the increase in the respective stress states, and then the difference it causes was calculated as percentage. As it is seen in Table 1 and 2, this parameter study showed that not all of the anisotropy parameters have significant impact on the interested stress states. Therefore, only four out of eight parameters, namely $\alpha_2, \alpha_4, \alpha_5$ and α_7, have been varied within this work.

Table 1: Significance of the anisotropy parameters on the plain strain area of YLD2000-2D

Deg. to RD	α_1	α_2	α_3	α_4	α_5	α_6	α_7	α_8
0° [%]	0.59	-1.49	0.68	-7.99	10.26	-1.32	0.00	0.00
45° [%]	0.00	0.00	-1.19	-1.74	-0.79	-0.21	3.95	0.28
90° [%]	1.08	6.31	-2.56	5.21	-8.60	0.25	0.00	0.00

Table 2: Significance of the anisotropy parameters on the biaxial stress area of YLD2000-2D

Deg. to RD	α_1	α_2	α_3	α_4	α_5	α_6	α_7	α_8
0° [%]	0.69	0.92	-3.11	-4.56	8.08	-1.77	0.00	0.00
45° [%]	-0.04	0.13	-2.49	-3.58	-1.04	-0.25	4.85	2.97
90° [%]	1.14	6.29	-3.47	-0.26	-1.74	-0.48	0.00	0.00

Some combinations of these parameters can result in non-realistic Lankford coefficients. In order to vary the corresponding Lankford coefficients around $\pm 10\%$, which reflects the real statistics, a preliminary study with one element simulations has been performed to determine the necessary amount of variation.

3.3 Fracture and Damage Modeling

CrachFEM is a sophisticated failure model comprising the evaluation of different failure types, such as ductile normal fracture caused by coalescence of microvoids and ductile shear fracture due to shear band localization [13]. The formulation of CrachFEM ductile shear fracture curve has been used to predict fracture strain, which is a function of the shear stress parameter θ, defined as

$$\theta = \frac{1 - k_s \cdot \eta}{\varphi} \qquad\qquad \varphi = \frac{\tau_{max}}{\sigma_{vM}} \qquad\qquad \tau_{max} = \frac{\sigma_1 - \sigma_3}{2} \qquad\qquad (11)$$

The ductile shear fracture strain is calculated by the following analytical function

$$\varepsilon_{SF}(\theta) = \frac{\varepsilon_{SF}^+ \cdot sinh\left(f \cdot (\theta^- - \theta)\right) + \varepsilon_{SF}^- \cdot sinh\left(f \cdot (\theta - \theta^+)\right)}{sinh\left(f \cdot (\theta^- - \theta^+)\right)} \qquad\qquad (12)$$

where the stress state parameters θ^+ and θ^- are computed from

$$\theta^+ = 2 \cdot (1 - 2 \cdot k_s) \qquad\qquad \theta^- = 2 \cdot (1 + 2 \cdot k_s) \qquad\qquad (13)$$

Thereby, the calculation of fracture curve is performed by fitting ε_{SF}^+, ε_{SF}^-, k_s, and f, but only ε_{SF}^+ was varied in the stochastic analysis, as the tested components tend to fail between plane strain and equibiaxial stress states. ε_{SF}^- is also given as a dependent parameter, for which the ratio between ε_{SF}^+ and ε_{SF}^- remains always the same. Even though CrachFEM is a very advanced and modular failure model, it lacks the ability to adapt the fracture curves to different mesh sizes. Therefore, the Generalized Incremental Stress State Model (GISSMO) [14] has been employed, which makes not only regularization w.r.t. element size but also material softening prior to reaching the fracture curve possible. The damage accumulation is based on an incremental formulation, which is expressed as

$$\Delta D = \frac{n}{\varepsilon_f} D^{(1-1/n)} \Delta \varepsilon_{vM} \tag{14}$$

where n is the damage exponent. The quantity ε_f serves as a weighting function representing the equivalent plastic strain to failure. It is given as a tabulated curve of failure strain vs. triaxiality, which is a measure of the corresponding stress state and expressed as

$$\eta = \frac{\sigma_H}{\sigma_V} = \frac{\sigma_1 + \sigma_2 + \sigma_3}{3\sigma_{vM}} \tag{15}$$

Depending on the damage threshold D_{crit}, the stress reduction is achieved by means of a modified Lemaitre's effective stress concept [15]. The highest possible accumulated damage value is hard coded to one and represents the element failure

$$\sigma^* = \sigma \left(1 - \left(\frac{D - D_{crit}}{1 - D_{crit}} \right)^m \right) \qquad \text{for } D \geq D_{crit} \tag{16}$$

where m is the fading exponent responsible for the amount of stress reduction. It is entered as a tabulated curve of the fading exponent vs. element size in order to control the dissipated energy during element fade-out. Fig. 5 shows the basis and regularized fracture curves w.r.t. element size.
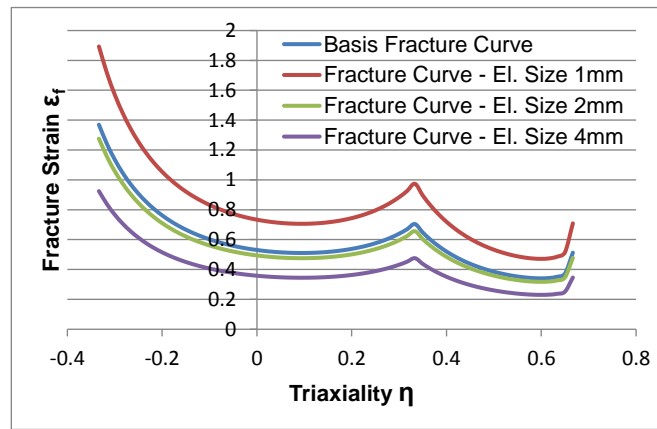
Fig.5: Basis and regularized fracture curves w.r.t. element size

4 Probabilistic Analysis & Global Sensitivity Analysis

4.1 Analytical Example

4.1.1 Ishigami Function

The methodology explained in section 2 has been tested on a non-monotonic and highly nonlinear function to see if iteratively increasing the number of sampling points increases the resulting sensitivity results. The Ishigami function has been used in many researches as a benchmark to test metamodeling performance and different sensitivity analysis methods [16, 17]. It has 3 parameters and 2 coefficients. The coefficients are usually taken as 7 and 0.1 for a and b, respectively. The parameters are uniformly distributed in the interval $[-\pi, \pi]$.

$$Y = f(X_1, X_2, X_3) = sinX_1 + asin^2X_2 + bX_3^4 sinX_1 \tag{17}$$

The considered number of points is 100, 250, and 500. The utilized metamodeling technique and the sampling algorithm are Radial Basis Function Networks and Space Filling algorithm, respectively. For the sake of simplicity, these techniques will not be explained, but it is referred to [2] for details. Normally, the metamodel accuracy is checked with some very well-known accuracy measures, such as the residual sum-of-squares in its square root form (RMS error), predicted sum-of-squares residual in its square root form (SPRESS), and coefficient of multiple determination (R^2). However, since the exact results of the sensitivity analysis are known, the Sobol indices are checked at each step. As the metamodel converges, i.e., its accuracy is at a certain level that it cannot be significantly improved further, the Sobol indices converge as well. Hence, the Sobol indices are compared with the analytically calculated sensitivities at each step, Table 3.

Table 3: Sobol's sensitivity indices computed on the metamodels generated with different number of sampling points

Method	S_1	S_2	S_3	S_{12}	S_{13}	S_{23}
Analytical	0.3119	0.4424	0	0	0.2437	0
RBF 100	0.4024	0.2914	0.00125	0	0.2736	0
RBF 250	0.3202	0.4242	0	0	0.2514	0
RBF 500	0.3194	0.4319	0	0	0.2455	0

It appears that 100 points are not enough to get converged results and obviously much better results can be obtained by adding 150 points. Another 250 points improve the results only by around 2%. Fig. 6 shows how the design space is filled iteratively with more sampling points while keeping the previous points and maintaining the equidistance w.r.t. the existing points.
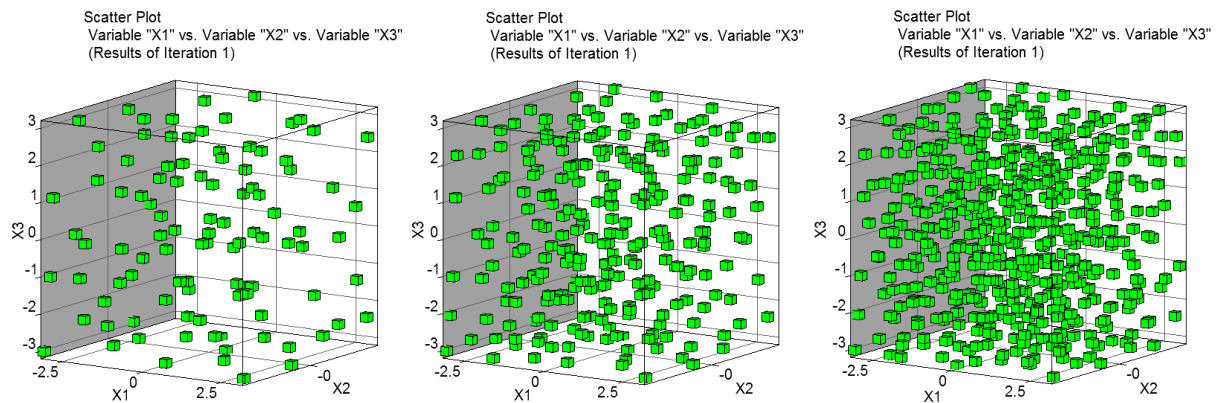
Fig.6: Design space iteratively filled with 100, 250, and 500 sampling points

4.2   Numerical Examples

In the following subsections, probabilistic analysis of two different components, side impact beam and a hat shaped profile, will be demonstrated. Several parameters have been considered for both forming and crash steps. Totally, 9 parameters for the quasi-static and 10 parameters for the dynamic analysis have been varied to account for the variation of experimental data. Normal distribution function reflecting the real statistics has been assigned to them, for which enough experimental data was available. The mean values have been taken from a previous work [7], where the parameters were optimized using experimental data. The parameters and their range of variation are given in Table 4. The range of variation corresponds to two times the standard deviation, which covers 95% of the confidence interval.

Table 4: Design parameters along with their variations corresponding to 95% confidence interval

Type	Parameter	Variation
Anisotropy	α_2	$\pm 2\%$
	α_4	$\pm 1\%$
	α_5	$\pm 2.5\%$
	α_7	$\pm 1.5\%$
Hardening	K	$\pm 5\%$
	n	$\pm 5\%$
Strain rate dependency	C	$\pm 20\%$
Fracture	ε_{SF}^+	$\pm 10\%$
Friction (forming)	μ_f	$\pm 20\%$
Friction (Crash)	μ_c	$\pm 20 - 30\%$

Apart from the variation of parameters, two different plasticity models, namely von Mises and YLD2000-2D, have been used in the analysis of the side impact beam to investigate the influence of yield locus on the failure prediction. The discretizations of forming and crash steps usually differ in

terms of the characteristic element length, as coarser meshes are used in crash simulations. This prevents the coincidence of in-plane integration points one-to-one while mapping forming history onto crash mesh. Moreover, it is desired to evaluate the variation of parameters on different element sizes. For this reason, 2 different discretizations have been employed in the crash step. A relatively simpler case with one plasticity model providing better results and one discretization has been investigated in the analysis of the hat profile. Fig. 7 shows the investigated process chains for quasi-static and dynamic cases.
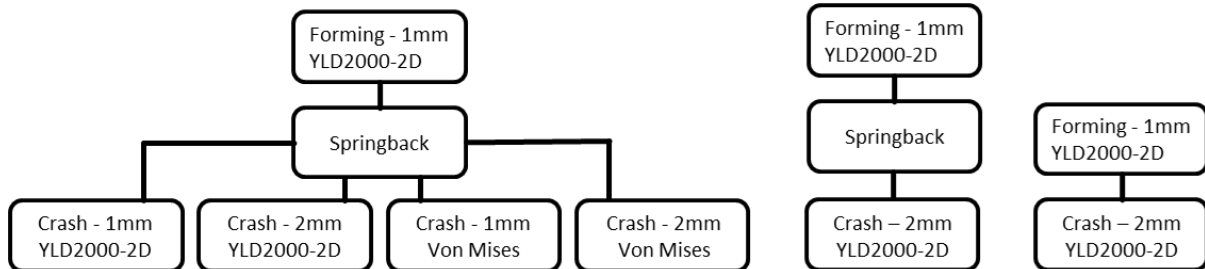
Fig.7: Overview of the process chains employed in this work. From left to right, quasi-static analysis of side impact beam, dynamic analysis of side impact beam and quasi-static analysis of hat profile

For the sake of computational cost, Belytschko-Tsay shell element with one in-plane integration point has been used in all simulations except springback analysis, where fully-integrated Belytschko-Tsay shell element is required.

4.2.1 Quasi-Static Three-Point Bending of Side Impact Beam & Hat Profile

Side impact beam is a suitable component to test under 3-point bending due to its localized failure. To perform the simulations as realistic as possible, all dimensions were taken from the tools and one of the formed parts. Comparison of the cross-sections at the middle of the part indicates that a significant amount of springback takes place, Fig. 8. Otherwise, mapping forming history properly would not be possible. This may affect the crashworthiness behavior.
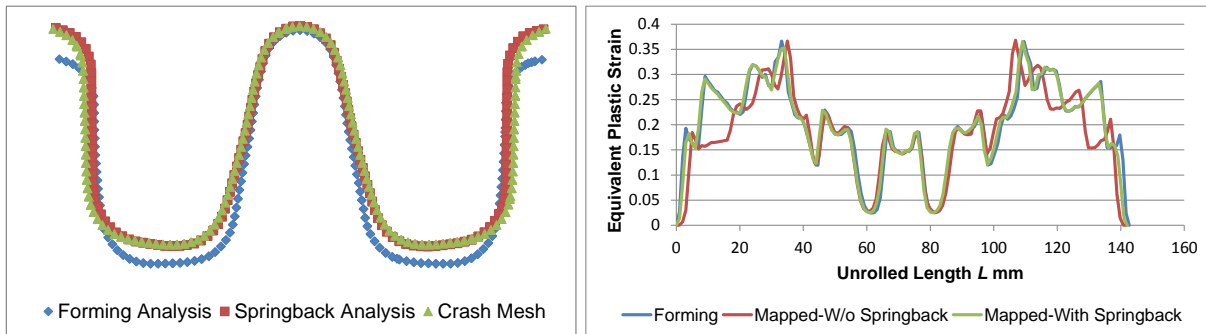

Fig.8: Cross-sectional view of side impact beam after forming and springback analyses, and crash mesh (left), mapped equivalent plastic strain with and without springback analysis (right)

Crash phenomenon is due to its highly non-linear nature more complex than forming, which makes it much harder to approximate via metamodels depending on the desired outputs. Moreover, not only deterministic variation but also random variation can cause in crash response. Hence, the metamodel accuracy have been checked for the crash related responses.
In the validation of crash tests, there are 4 criteria to be fulfilled
- Deformation behavior
- Fracture location (if exists)
- Force vs. Displacement curves / Energy absorption
- Fracture timing
With the optimized values obtained in [7], the first three criteria have been fulfilled for the quasi-static simulations of the side impact beam. The force vs. displacement curves are in good agreement except for the abrupt force drop, Fig. 9, caused by edge crack, which requires a special fracture model and is not in the scope of this work. As it is also proved in the same work that the edge crack does not influence the plastic strain accumulation at the fracture location, it has not been considered in the crash simulations.
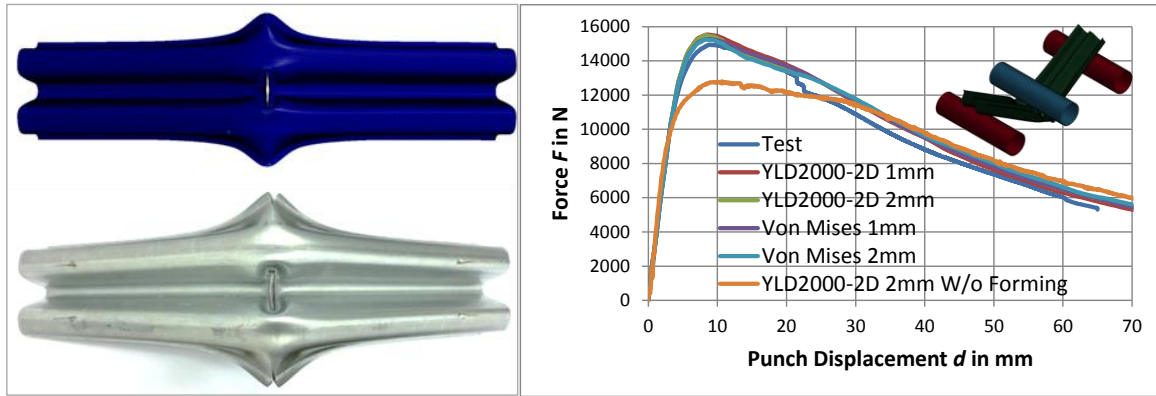
Fig.9: Side impact beam after three-point bending test and the computed force vs. displacement curves with different yield loci

As for the fourth criterion, the resulting displacements up to fracture are close to the test results, Table 5. Thanks to the regularized fracture curve and the corresponding fading exponents, different discretizations provide similar results. YLD2000-2D coupled with GISSMO appears to estimate the displacement up to fracture better, but it should be pointed out that there are some assumptions made in the optimization of damage parameters that might not be in favor of von Mises.

Table 5: Punch displacement up to fracture obtained with different yield loci and element sizes

Method	El. Size-1mm	El. Size-2mm
YLD2000-2D	57mm	56mm
Von Mises	52mm	48mm
Tests	53-61mm	

The metamodel accuracy has been checked with different measures and Sobol indices for the desired responses. For the probabilistic analysis of quasi-static three-point bending tests, sampling points starting with 20 have been increased by 8 in each step up to 100. In case of using YLD2000-2D and 1mm element size for both forming and crash steps of the process chain, around 40 sampling points were found enough for the Sobol indices to converge for the displacement up to fracture, whereas no significant change was observed after 20 sampling points for the crash analysis with 2mm element size. The most important parameter was already clear with 20 points, though. This indicates that the relation between variables and responses is quite linear and the added points are mainly to compensate the residuals stemming from outliers. The displacement up to fracture is the displacement, at which the damage accumulation reaches one for an element at the fracture location. For an element to be deleted, 60% of the through-thickness integration points must fail, but it is not a hard-coded feature of GISSMO and should be adjusted according to the deformation and fracture behavior. As the first element to be deleted and its last integration point to fail might change from one simulation to another, evaluations cannot be performed on a predefined element or node. This challenge has been overcome by the implemented perl scripts extracting all necessary information automatically for all simulations. Fig. 10 shows the respective global sensitivity and stochastic contribution analysis results with different number of sampling points for the displacement up to fracture, where the distribution functions of the input parameters are taken into account for the latter. This difference makes stochastic contribution analysis more important for probabilistic analysis. Due to dominant influence of one parameter, the results seem almost the same but might differ depending on the evaluated response.
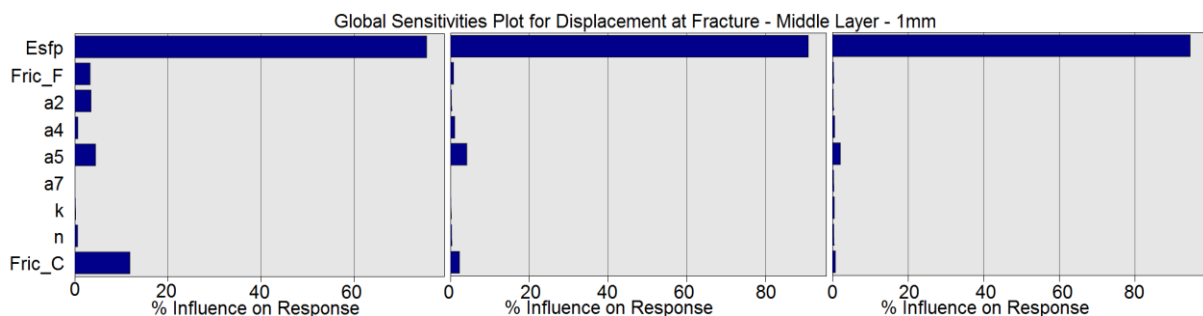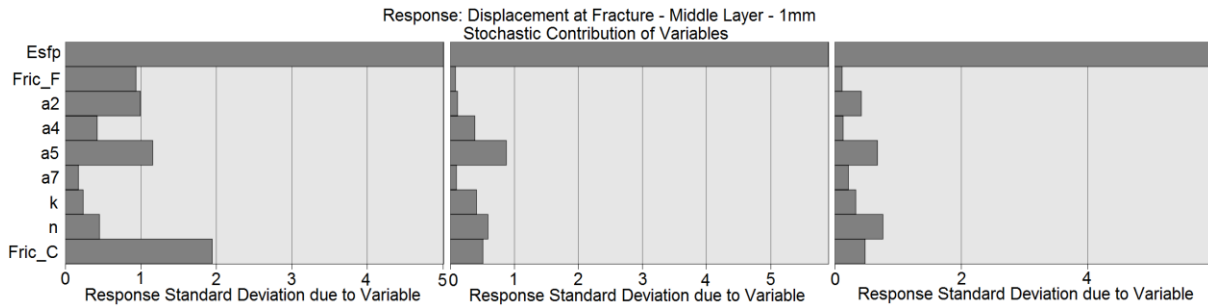
Fig.10: From left to right, top: global sensitivity analysis with 20, 52, and 100 sampling points bottom: stochastic contribution analysis with 20,52, and 100 sampling points for the side impact beam

It is plausible that the fracture curve turns out to be the most important variable. On the other hand, both analyses reveal that the variation of yield curve is not as significant as expected. However, the variation of the displacement up to fracture should be considered together with the variation of the force vs. displacement curve because none of them alone suffices to validate a crash test in the presence of fracture. As seen in Fig. 9, the force vs. displacement curve has only one peak, which can be used to reveal the relationship between the maximum reaction force and parameters. The multi-response plot, Fig. 11, is the combination of the Sobol indices for the maximum force and displacement up to fracture. It must be kept in mind that no weighting factor is assigned to the responses. The result of ANOVA, Fig. 11, represents the absolute change of the mean value of the maximum reaction force. It can be concluded from the superior metamodel accuracy (RMS = 0.0879%) and very tight confidence intervals that there is a completely linear relationship between the parameters and the maximum reaction force. Thus, the importance ranking according to ANOVA is reliable. It is noticeable that the influence of the anisotropy parameter α_5 is higher than almost all parameters except K, the strength coefficient of the Swift's law. According to the results of the parameter study given in 3.2.1, the importance of α_5 can be explained by the loading and the orientation of the component.
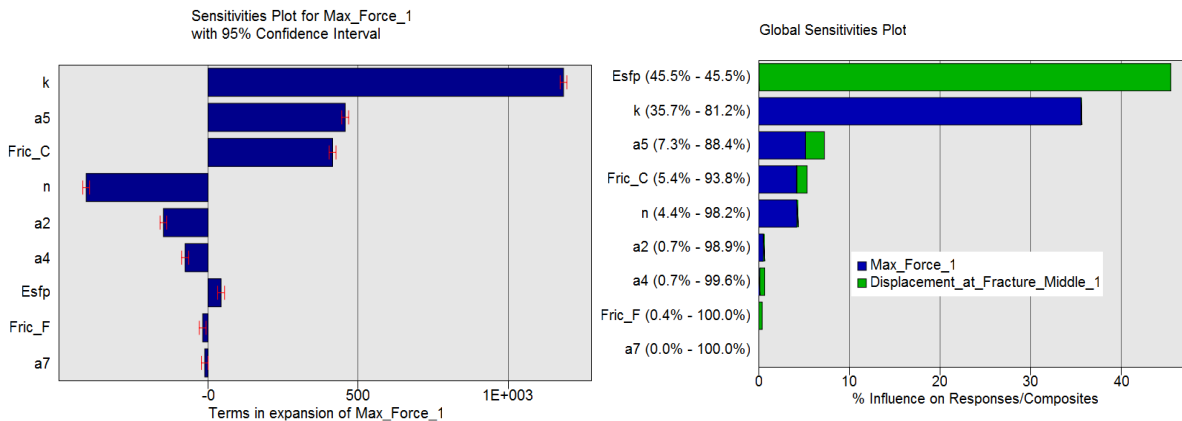

Fig.11: The importance ranking of variables for the maximum force acc. to ANOVA (left) and global sensitivity analysis for both maximum reaction force and displacement up to fracture (right) for the side impact beam

The distribution of the displacement up to fracture, Fig. 12, for different elements sizes and yield loci helps to quantify its variation w.r.t. the variation of all parameters. Being the most important parameter for this response and causing more than 90% of its variation, the quantification can be based solely on the variation of the fracture curve. ±10% variation of the fracture curve causes ±20-30% and ±40-50% variation of the fracture displacement for 1mm and 2mm element sizes, respectively. The percentages are computed considering 95% confidence interval for both parameters and responses. These results indicate the importance of reducing uncertainty in the methods used for identifying material constants, especially fracture strains.
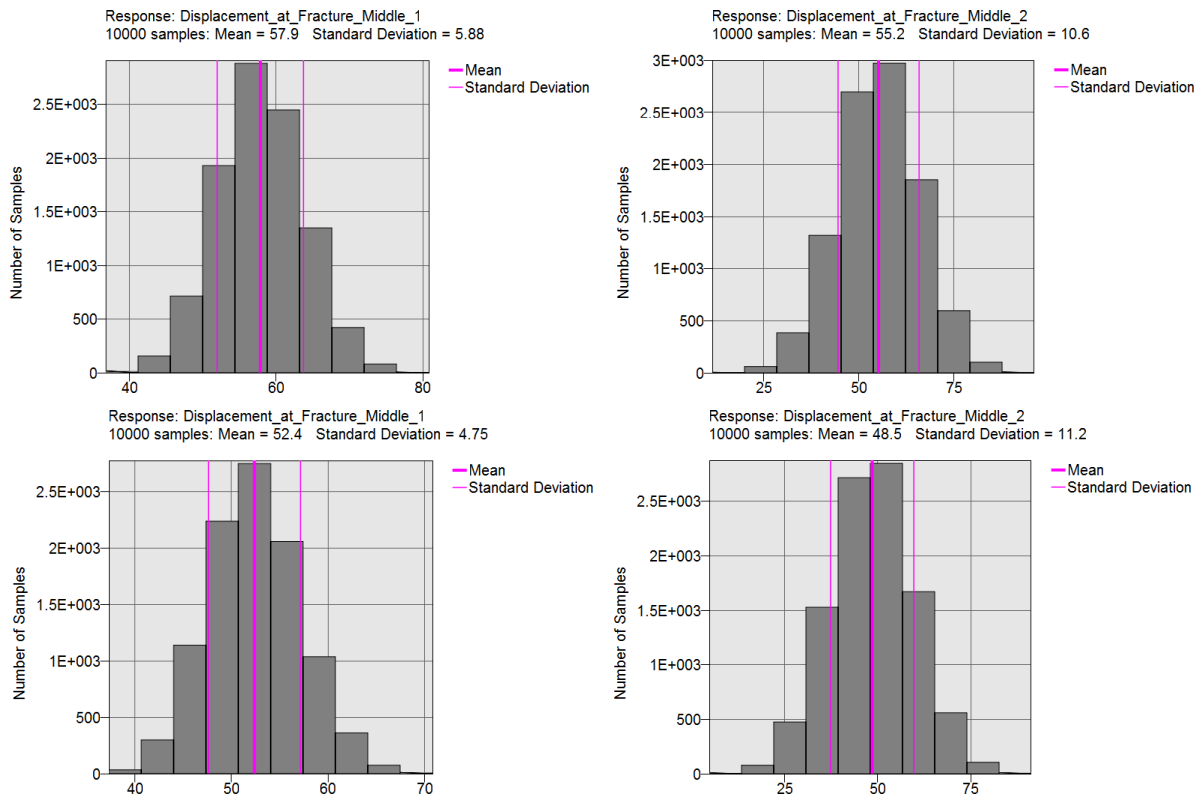
Fig.12: Statistical measures along with the distributions for the response "Displacement up to fracture". Top: YLD2000-2D with 1mm and 2mm. Bottom: Von Mises with 1mm and 2mm

The results are similar for the same response with von Mises (crash), but the anisotropy coefficients are even less significant indicating that their variations do not cause high variation in maximum plastic strain during the forming step at the expected fracture location. Examining the maximum plastic strain at different layers in the forming step points to the same fact, Fig. 13 shows the global sensitivity analysis results for the max plastic strain on both lower and middle layers at the expected fracture location. The variation in the forming friction coefficient is more important than the material related parameters. Nevertheless, the amount of variation is by up to 4% negligible. This low amount of variation is probably a result of the manufacturing process known as "Crash Forming", where no blankholder is employed. It is expected to have higher amount of variation in a deep drawn part.
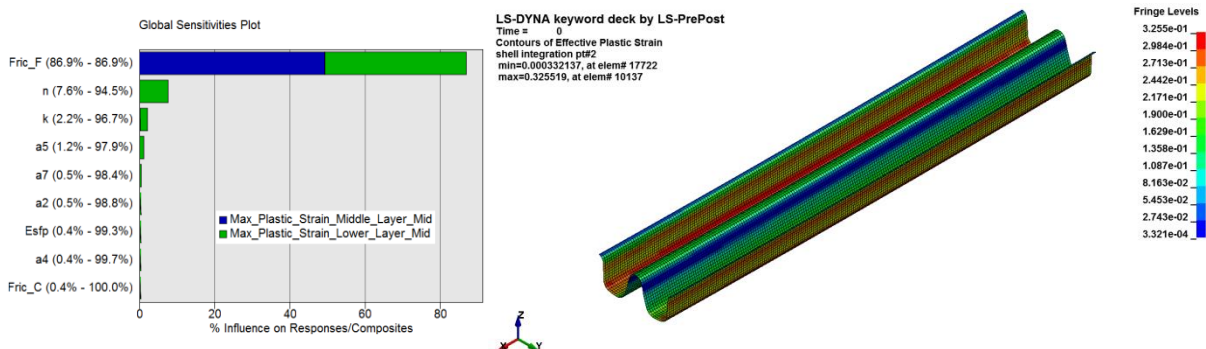

Fig.13: Combined Sobol indices for the maximum plastic strain at the expected fracture location on different layers (left), and contour plot of effective plastic strain at the upper layer after forming (right)

Another part having the geometry of hat profile has been tested under three-point bending to see if the results are similar. The part is formed through bending; therefore, the plastic straining occurs only at its corners. Tested with the optimized parameters, the computed force vs. displacement curve is in good agreement with the tests, Fig. 14. The number of integration points to fail before an element is removed from the FE model has been set to 2 out 5 instead of 3, where the latter results in very late failure. This occurs due to distinct fracture behavior of the critical elements.
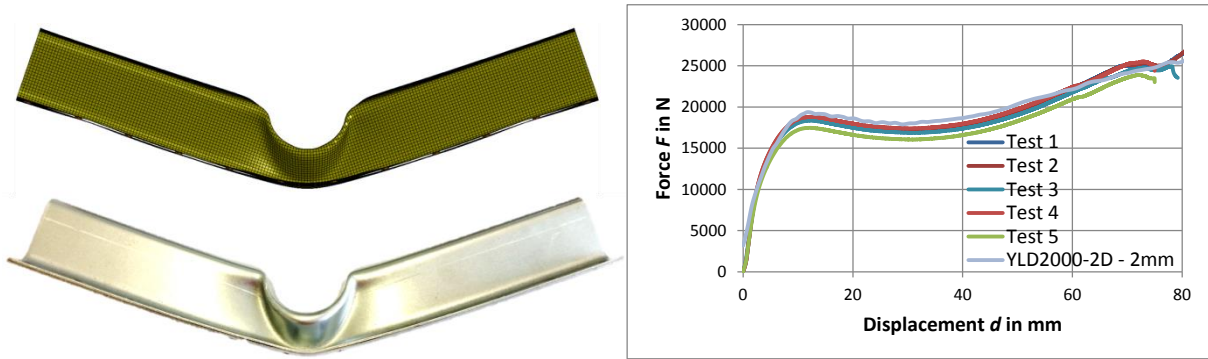
Fig.14: Simulation and test in deformed configuration, and the force vs. displacement curves

The same amount of variation as used for the side impact beam has been applied to all variables except the friction coefficient, which has been varied around ±30% instead of ±20%. Due to poor accuracy of the metamodel, the first 20 simulations have been thoroughly investigated. Unusual deformation mode arose as the main cause of outliers. Performing a sensitivity analysis on the distance between the marked nodes seen in Fig. 15 brought out that less than a certain amount of friction leads to erroneous deformation, Fig. 15.
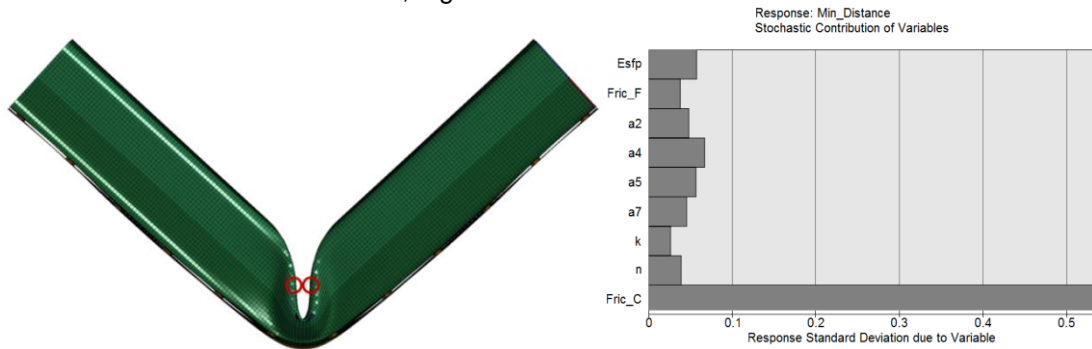

Fig.15: Abnormal deformation due to lack of sufficient friction (left), stochastic contributions of the variables to the distance between the marked nodes (right)

On account of this reason, the variation interval of the friction coefficient has been changed and the simulations have been repeated with new sampling points. The sampling points have been iteratively increased up to 52 points. No significant improvement of metamodel accuracy has been observed, as 20 sampling points were already sufficient to approximate the linear relationship between the parameters and the desired responses. Applying the optimized parameters, 2mm element size and YLD2000-2D throughout the process chain, the displacement up to fracture becomes around 70mm, which falls into the variation of the tests that are between 68 and 73mm. The stochastic contribution analysis of the hat profile verifies the previous results of the side impact beam, Fig. 16. On the other hand, the variation of the displacement up to fracture is around ±20%.
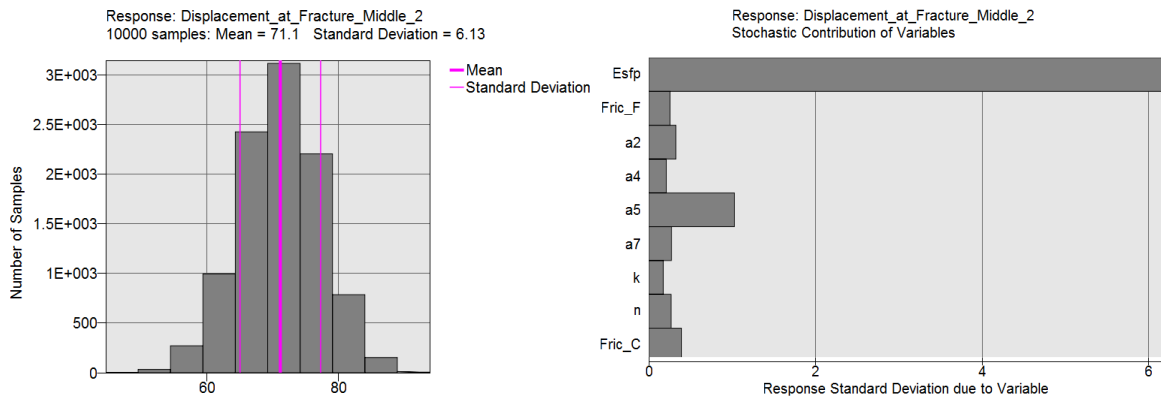

Fig.16: Metamodel based Monte Carlo analysis for the displacement up to fracture (left), stochastic contributions of the variables to the displacement up to fracture (right)

The standard deviation is almost half of that found with the same element size and yield locus for the side impact beam. Comprised of the elements having the same size, the same fracture curve has been used for both parts. In other words, the same boundaries for the fracture strain have been applied through the whole triaxiality range. On the other hand, folding behavior at the fracture location is different. The ability of the selected element type to describe the folding behavior might also contribute to the difference between the standard deviations. Under the light of these facts, the critical elements have been compared with each other in terms of plastic strain and damage accumulation. Since the same damage and fading exponents have been used for the considered integration points of the critical elements, only strain path can alter the damage accumulation and thereby the fracture strain. The damage accumulation is based on the distance between the fracture curve and the accumulated equivalent plastic strain. If the strain path is completely linear, then fracture occurs right on the fracture curve, but it might happen over or under the fracture curve for non-linear strain paths. The strain paths of the critical through-thickness integration points, shown in Fig. 17, differ in terms of evolution and final loading state. The damage accumulation is therefore distinct and allows more straining for the critical element of the hat profile. Moreover, based on the assumption that the critical integration points of all simulations have similar strain paths, the variation of the fracture curve by ±10% encompasses a more critical interval of the accumulated damage, which then together with the allowance of more straining gives rise to the difference in the standard deviations.
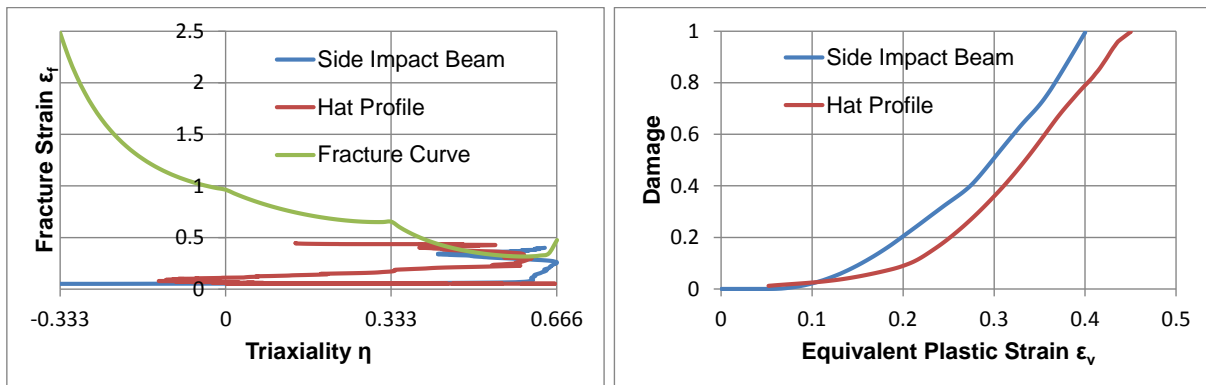

Fig.17: Strain paths (left) and damage accumulation of the critical integration points (right)

The influence of the parameters on the reaction force has been investigated for the hat profile, as well. The force vs. displacement curve is more complex and has more than one peak defining different deformation steps. Thus, the maximum reaction force does not seem to be suitable for determining the influence of parameters. The Mean Square Error (MSE) for all points forming the curve has been used for this reason. The global sensitivity analysis results of the MSE and the maximum reaction force have been compared with each other to support the idea. The maximum reaction force occurs after failure. As seen in Fig. 18, the three most important parameters are the hardening parameters and friction coefficient as expected, but the ranking is different. The results demonstrate that the influence of the process related parameters is not constant throughout the whole deformation process.
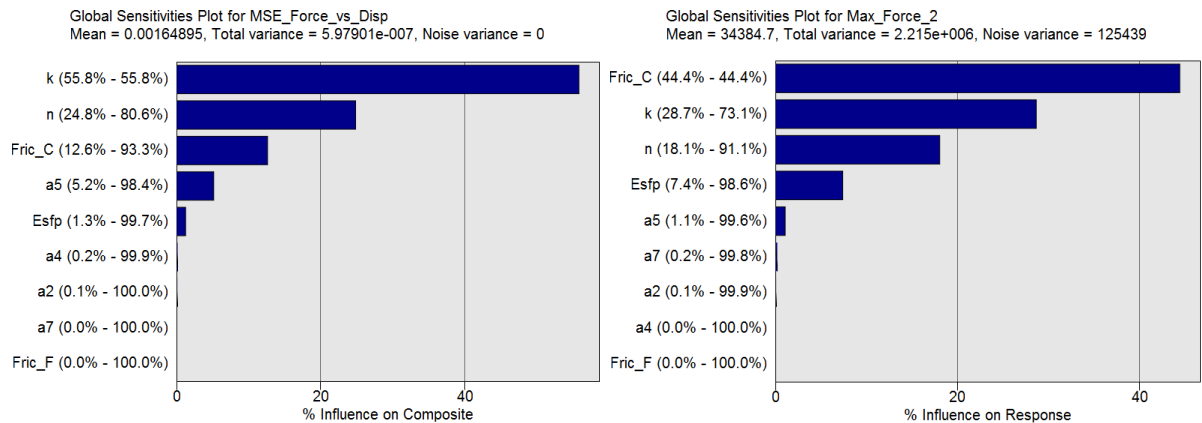

Fig.18: Global sensitivity analysis for the MSE of the force vs. displacement curve (left) and the maximum reaction force (right)

4.2.2 Dynamic Three-Point Bending of Side Impact Beam

The dynamic tests have been conducted by a drop hammer. The predefined mass drops from a predefined height along two guiding rods onto test sample. Compared to the quasi-static testing, the speed is relatively high. The respective force vs. displacement curve does not allow detecting the punch displacement at which failure takes place. In order to narrow it down, the minimum amount energy necessary to cause failure has been determined by trial and error method. It should be kept in mind that the theoretical calculated velocity might not match the real velocity due to friction along the guiding rods.

Although the same amount of energy was applied, 3 out of 10 samples did not fail. The failure is estimated to take place between 67 and 72mm. It has also been observed that a significant amount of variation exists concerning the maximum punch displacement. Table 6 shows the maximum punch displacement of all tests and whether or not failure has occurred.

Table 6: Overview of tests considering failure along with maximum punch displacement

Sample	Failure	Max. Punch Displacement (mm)
1	Yes	69.7
2	No	64.9
3	No	66.9
4	Yes	70.2
5	Yes	71.3
6	Yes	72.5
7	No	73.9
8	Yes	71.6
9	Yes	67.9
10	Yes	68.3

Assessing the variation of the displacement up to fracture requires all simulations to have failure. Depending on the set of sampling points, some combinations might not cause failure if the same amount of energy is applied in the numerical analysis, especially when the fracture curve is raised. For the Monte Carlo analysis, the amount of potential energy has been increased by about 30%. The displacement up to fracture has been checked for both nominal and increased potential energy. It has been observed that the difference is negligible. The simulation performed by means of the optimized and fitted parameters fails at 64mm and the maximum punch displacement is 68 mm. 15% difference between the quasi-static and dynamic analysis in the displacement up to fracture stems clearly from the consideration of strain rate dependency. The parameters of the failure model might also be strain-rate dependent, which requires further testing to establish and has not been taken into account in this work. Fig. 19 shows the tested and computed force vs. displacement curves.
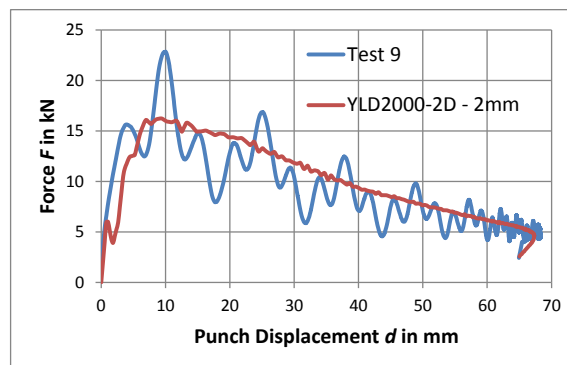

Fig.19: Force vs. displacement curves obtained from a dynamic 3-point bending test and a respective simulation

Starting with 20 sampling points and adding more iteratively up to 52, around 30 sampling points have been found sufficient to construct a good metamodel. The resulting statistics of the displacement up to fracture do not differ much from the quasi-static simulations except the significant increase in the mean value. As expected, the importance ranking of the variables is also the same, Fig. 20. As for the maximum punch displacement, its standard deviation as a percentage is in very good agreement with

the test results, Fig. 20. The prominent outcome is the significance of the fracture curve for the energy absorption. Depending on the number of deleted elements, it can be as important as some of the hardening related parameters.
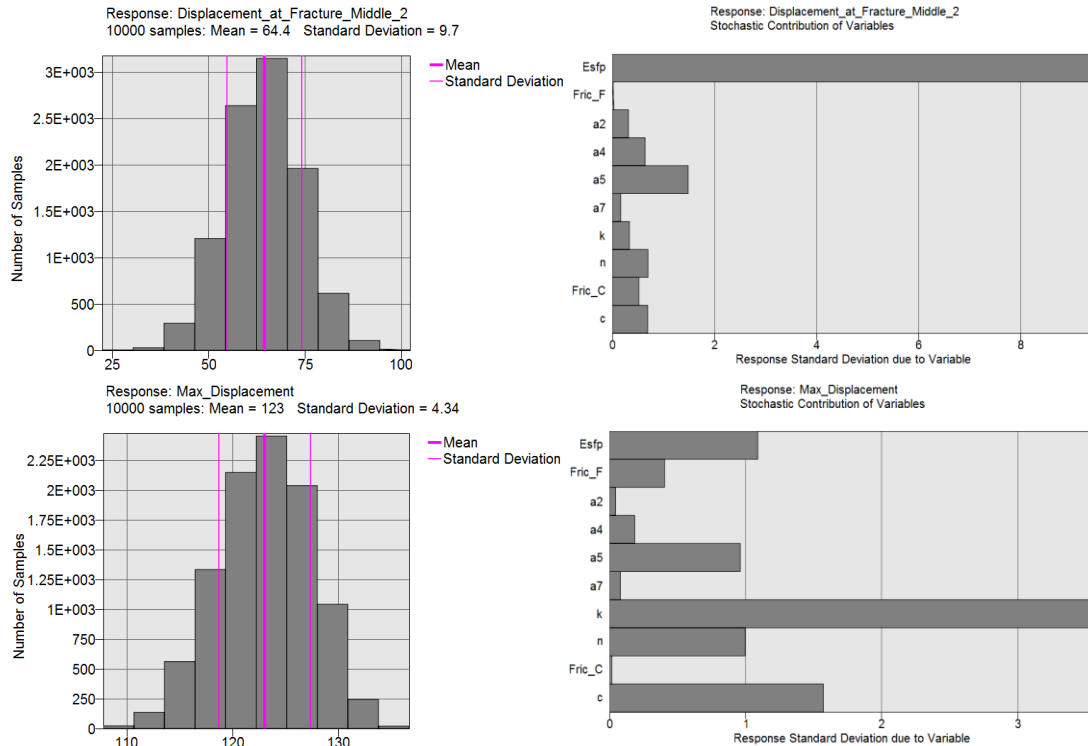

Fig.20: Top: Metamodel based Monte Carlo analysis for the displacement up to fracture (left) and stochastic contributions of the variables (right). Bottom: Metamodel based Monte Carlo analysis for the maximum punch displacement (left) and stochastic contributions of the variables (right)

5 Summary

Material scatter is evident in all kinds of mechanical tests. However, it is due to not only the inhomogeneity of materials but also the methods used for obtaining data. This situation causes the questioning of results in terms of reliability. Yet, it has not been paid enough attention. In order to account for the scatter, processes must be simulated by taking stochastic aspects into account. In this work, a methodology has been developed to perform probabilistic analysis on the process chain "Forming to Crash", and it has been tested on two different parts, namely side impact beam and hat profile, under both quasi-static and dynamic conditions. The results show that the variation of material and process parameters leads to much higher variation in the outputs. The fracture curve turns out to be the most important parameter concerning the displacement up to fracture for all testing conditions, material models and element sizes, whereas the relative insignificance of the parameters pertaining to the yield curves is an unexpected but crucial outcome of this work. On the other hand, validation of crash processes requires good approximation of energy absorption behavior, where the parameters describing the hardening behavior of materials become the vital ones. Moreover, the variation of hardening parameters has been kept relatively small to reflect only the variation of yield curves, but it is intended to increase the variation range of the extrapolation related parameters in further research, so that not only the variation of the experimental yield curves but also the variation caused by different modeling approaches will be taken into account.

The dominant influence of the fracture curve lets its variation be quantified on the variation of results. Utilizing two different parts and simulating the process chain under the same conditions, i.e. the same element size, material model, and loading, revealed that this quantification cannot be thought as constant because of its high dependency on the strain path and thereby the damage accumulation. Consequently, ±10% variation of the fracture curve caused an amount of variation between ±20% and ±50% on the displacement up to fracture depending on the element size and the tested part. It should be kept in mind that the meshes used in this work are quite fine and it is usually preferred to use coarser discretization for crash simulations, which might further increase the variation of results.

6 Literature

[1] Reuter, R.; Gärtner, T.: Stochastische Crashsimulation mit LS-DYNA am Beispiel des Kopfaufpralls nach FMVSS 201, 1999, 17. CAD-FEM Users Meeting, Sonthofen

[2] Stander, N.; Roux, W.; Goel, T.; Eggleston, T.; Craig, K.: LS-OPT User's Manual, 2012

[3] Hohage, B.; Förderer, A.; Geißler, G.; & Müllerschön, H.: Global Sensitivity Analysis in Industrial Application with LS-OPT, 2010, 9. LS-DYNA Forum, Bamberg

[4] Myers, R.; Montgomery, D.: Response Surface Methodology, 1995, Process and Product Optimization using Designed Experiments, Wiley

[5] Sobol, I.: Global Sensitivity Indices for Nonlinear Mathematical Models and Their Monte Carlo Estimates, 2001, Mathematics and Computers in Simulation 55, pp. 271-280

[6] Saltelli, A.; Ratto, M.; Andres, T.; Campolongo, F.; Cariboni, J.; Gatelli, D.; Saisana, M.; Tarantola, S.: Global Sensitivity Analysis: The Primer, 2008, John Wiley and Sons Inc.

[7] Özarmut, B.; Richter, H.; Brosius, A.: Parameter Identification of a Damage Model for the Process Chain "Forming to Crash", 2014, 3. International Conference on Recent Trends in Structural Materials, Pilsen

[8] Johnson, G. R.; Cook, W. H.: A constitutive model and data for metals subjected to large strains, high strain rates and high temperatures, 1983, Proceedings of the Seventh International Symposium on Ballistics, pp. 541-547, Hague

[9] Kang, W.; Cho, S.; Huh, H.; Chung, D.: Modified Johnson-Cook model for vehicle body crashworthiness simulation, 1999, Int. J. Vehicle Design 21, pp. 424-435

[10] Yu, H.; Guo, Y.; Lai, X.: Rate-dependent behavior and constitutive model of DP600 steel at strain rate from 10^{-4} to 10^{3} s^{-1}, 2009, Materials and Design 30, pp. 2501-2505

[11] Gerlach, J.; Keßler, L.: Impact of Advanced Material Models on Forming and Part Properties, 2003, EuroPAM Conference, Mainz

[12] Barlat, F.; Brem, J.C.; Yoon, J.W.; Chung, K.; Dick, R.E.; Choi, S.H.; Pourboghrat, F.; Chu, E.; Lege, D.J.: Plane stress yield function for aluminum alloy sheets–part 1: theory. Int. J. Plasticity, 19, 2003, pp. 1297-1319

[13] Gese, H.; Oberhofer, G.; & Dell, H.: Consistent Modeling of Plasticity and Failure in the Process Chain of Deep Drawing and Crash with User Material Model MF-GenYld + CrachFEM for LS-Dyna, 2007, 6. LS-DYNA Anwenderforum, Frankenthal

[14] Neukamm, F.; Feucht, M.; Haufe, A.: Considering damage history in crashworthiness simulations, 2009, 7. European LS-Dyna Conference, Salzburg

[15] Lemaitre, J.: A Continuous Damage Mechanics Model for Ductile Fracture, 1985, Journal of Engineering Materials and Technology 107, pp. 83-89

[16] Reuter, U.; Liebscher, M.: Global sensitivity analysis in view of nonlinear structural behavior, 2008, 7. LS-DYNA Anwenderforum, Bamberg

[17] Reuter, U.; Mehmood, Z.; Gebhardt, C.: Using LS-OPT for meta-model based global sensitivity analysis, 2011, 8. European LS-DYNA Conference, Straßburg